Insect science

Insect Science (2023) 0, 1–11, DOI 10.1111/1744-7917.13173

ORIGINAL ARTICLE

Ligand dose-dependent activation of signaling pathways through the gustatory receptor *Nl*Gr11 linked to feeding efficacy in *Nilaparvata lugens*

Wei-Wen Chen[1], Kai Lin[1], Jun Lv[1], Qin Su[1], Meng-Yi Zhang[1], Kui Kang[2] and Wen-Qing Zhang[1]

[1]*State Key Laboratory of Biocontrol and School of Life Sciences, Sun Yat-sen University, Guangzhou, China* and [2]*College of Biology and Agriculture, Zunyi Normal University, Zunyi, Guizhou Province, China*

Abstract Insects often face both conditions with sufficient nutrients and conditions of undernutrition in the field. Through gustatory receptors, insects sense nutrients and regulate their physiological functions such as feeding and reproduction. However, it remains unclear whether signaling pathways activated by gustatory receptors depend on the concentration of nutrients and whether the difference in signaling pathways directly affects insects' physiological functions. Herein, we found that a sugar gustatory receptor, *Nl*Gr11, from the brown planthopper (BPH), *Nilaparvata lugens*, activated G protein-coupled signaling and ionotropic pathways when bound to high galactose concentration. BPHs subsequently demonstrated longer feeding times, feeding loads, and higher vitellogenin (*Nl*Vg) expression than BPHs exposed to high galactose concentrations, which only activated the ionotropic pathway. For the first time, our findings link plant nutrient conditions, signaling pathways activated by nutrients, and their gustatory receptors, and nutrient dose-dependent feeding efficacy and vitellogenin (Vg) expression in an insect. This will help us to better understand the molecular mechanism for insect feeding strategies on plants at different stages of nutritional conditions.

Key words feeding efficacy; galactose; G protein-coupled signaling pathway; insect gustatory receptor; ionotropic pathway

Introduction

Statistically, more than 50% of a million known insect species are phytophagous (Ortego, 2012). The normal growth, development, and reproduction of herbivorous insects depends on finding suitable host plants and obtaining adequate nutrients such as sugars and amino acids from their host plants (Facknath & Lalljee, 2005). However, insects often face conditions of either sufficient nutrients or undernutrition in the field. Nutrient content can directly affect the feeding behavior, growth, and reproduction of herbivorous insects. For example, when *Nilaparvata lugens* (the brown planthopper, BPH) fed upon *Oryza sativa* plants with nitrogen deficiency, the probing number increased significantly and the feeding speed and quantity decreased (Sōgawa, 1982). As the nitrogen content of the plants increased, the growth rate, lifespan, and fecundity of the insects increased (Fischer & Fiedler, 2000; Bi *et al.*, 2001; Nevo & Coll, 2001). The sucrose intake of *Psyttalia lounsburyi* increased with increasing sucrose concentration (Williams *et al.*, 2015). *Aedes albopictus* fed with a high sucrose concentration showed a higher mean fecundity rate than *A. albopictus* fed with a low sucrose concentration and had higher daily biting rates (Naziri *et al.*, 2016).

Correspondence: Wen-Qing Zhang, State Key Laboratory of Biocontrol and School of Life Sciences, Sun Yat-sen University, Guangzhou 510275, China. Email: lsszwq@mail.sysu.edu.cn

Insect gustatory receptors play crucial roles in sensing and recognizing nutrients in plants (Chapman, 2003; Xu, 2020). Two potential mechanisms of signal transduction are found after sensing taste substances. The first mechanism is the ligand ion-gated channel, exemplified by *Bombyx mori* Gr9 (*Bm*Gr9) and *Bm*Gr10, that causes a direct cation influx into the cytoplasm in response to fructose and *myo*-inositol stimulation, respectively (Sato *et al.*, 2011; Kikuta *et al.*, 2016). The second mechanism is the G protein-coupled signaling pathway activated by *N. lugens* Gr11 (*Nl*Gr11), a sugar gustatory receptor, in response to galactose (Chen *et al.*, 2021). Moreover, the nutrient content of plants is not constant, with sugar levels, for example, being temporally and spatially regulated in the plant (Lastdrager *et al.*, 2014). Using rice as an example, as the plants begin to mature the soluble sugar content increases to its highest level (Li *et al.*, 2013). The glucose concentration of rice plants increases from the seedling stage and then decreases at the mature stage (Lin *et al.*, 2018). Although gustatory receptors can regulate the feeding loads of insects (Miyamoto *et al.*, 2012; Ai *et al.*, 2022), it remains uncertain whether signaling pathways activated by gustatory receptors rely on the concentration of nutrients in plants, and whether the difference in signaling pathways directly influences insects' physiological functions.

Rice is a primary staple food crop and a source of calories for billions of people worldwide (Du *et al.*, 2009). The BPH, *N. lugens* (Stål), is the most destructive insect pest of rice and severely threatens rice yield (Yang & Zhang, 2016). Galactose has been previously identified as a ligand of *Nl*Gr11, a sugar gustatory receptor in BPH. We observed that galactose resulted in dose-dependent Ca^{2+} increases at concentrations ranging from 5 to 50 mmol/L and showed a saturatable response at 50 mmol/L (Chen *et al.*, 2019). In another study, we found that galactose-*Nl*Gr11 promoted AKT phosphorylation via the insulin receptor and G$\beta\gamma$, and inhibited adenosine monophosphate-activated protein kinase (AMPK) phosphorylation through the protein kinase B (AKT)-phosphofructokinase (PFK)-ATP signaling cascade, and finally mediated the fecundity of BPHs (Chen *et al.*, 2021). Herein, we investigated distinct signaling pathways when galactose was bound to *Nl*Gr11 (galactose-*Nl*Gr11) *in vitro* and *in vivo*, as well as galactose dose-dependent feeding efficacy and *Nl*Vg expression of BPHs. We demonstrated that galactose-*Nl*Gr11 activated either one or both of the ionotropic and G protein-coupled signaling pathways, based on galactose concentration. We also determined that with the activation of G protein-coupled signaling triggered by high galactose concentrations, the BPHs demonstrated fewer feeds, longer feeding times, and greater feeding loads, as well as higher *Nl*Vg expression.

Materials and methods

Cell culture, storing, and maintenance

A stable *Nl*Gr11-transfected *Sf*9 cell line, *Nl*Gr11-*Sf*9, was established in our recent study (Chen *et al.*, 2019). Briefly, the polymerase chain reaction (PCR) product of the open reading frame (ORF) was digested with *Hind*III and *Eco*RI and then ligated into the pIZ/V5-His vector. Subsequently, *Sf*9 cells were transfected with 200 ng of the plasmid construct pIZ/*Nl*Gr11 and 6 μL of the FuGENE HD transfection reagent in 100 μL of medium per well. After successful transfection, *Nl*Gr11-*Sf*9 stable cell lines were established using a Zeocin-containing medium. The final concentration of Zeocin to maintain the cells was 50 μg/mL.

After the cell lines were successfully established, during the logarithmic growth period cells were taken and gently washed with medium to separate them from the culture dish and then centrifuged for collection. The medium was then removed and 1 mL of cryopreservation solution (containing 10% DMSO and 10% BSA) was added and gently mixed to resuspend the cells for transfer to the cryopreservation tube. Lastly, the cryopreservation tube was placed in a cryopreservation box containing isopropanol, precooled to 4°C, and then transferred to liquid nitrogen for long-term storage after overnight storage at −80°C.

To resuscitate the frozen cells, the cryopreservation tube was taken out of liquid nitrogen and placed in a water bath held at 37°C for 2−3 min. After the cryopreservation solution had dissolved, the cryopreservation solution was transferred to a culture dish and medium preheated to 28°C was slowly added. After 24 h the medium was renewed and the culturing of the cells continued. Cells that have recovered the growth state and have passed through 4 generations can be used in the experiment.

Insect rearing

The *N. lugens* (BPH) populations used in this work were originally collected in Guangdong Province, China, in 2012. All BPHs were mixed reared in a walk-in chamber at 26 ± 1°C under a photoperiod of 16 : 8 h (light : dark) and at a relative humidity level of 80% ± 10% on susceptible rice seedlings (of rice variety Huang Huazhan).

Chemicals

Galactose was purchased from Beijing Dingguo Changsheng Biotech. Co. Ltd (Beijing, China), with purity ≥98.5%. Fluo-4 AM was purchased from Invitrogen (Waltham, MA, USA), guanosine 5′-*O*-(2-thiodiphosphate) (GDP-βS) and deoxycholate (DOC) were purchased from Sigma-Aldrich (St. Louis, MO, USA). Manidipine 2HCl, U73122, and neomycin were purchased from Selleck Chemicals (Houston TX, USA). 2-Aminoethoxydiphenylborate (2-APB) and adenophostin A were purchased from Calbiochem (San Diego, CA, USA).

Calcium imaging assay

Calcium imaging was performed using a modification of a previously described method (Chen *et al.*, 2019). Briefly, the medium was removed and the cells were washed with Hank's buffer (with Ca^{2+}) or D-Hank's solution (without Ca^{2+}). Cells were loaded with calcium indicator Fluo-4 AM (2 mmol/L) in 2 mL of Hank's buffer or D-Hank's buffer and then incubated at 28°C for 40 min. Subsequently, the cells were washed twice with Hank's buffer or D-Hank's buffer to remove excess Fluo-4 AM and were covered with 2 ml of fresh buffer. Fluorescence imaging was performed using a confocal laser scanning microscope (Leica, Wetzlar, Hesse, Germany). Images were recorded every 3 s for 120 s following the addition of the test solutions. According to the results of our previous research (Chen *et al.*, 2019), unsaturated galactose concentrations (5, 10, 20, 40, and 45 mmol/L) and the saturated concentration (50 mmol/L) were chosen as test concentrations. Fluorescence intensity was recorded for identified cells in each image using the Metafluor® imaging system (Leica). The test solution was added at the 30th second of data recording and then recording continued for another 90 s. All the values of fluorescence intensity were normalized to the first value, so the first value was set to 1. The normalized value was relative luminosity, which represents the level of intracellular Ca^{2+}. Six bottles of cells were detected for each treatment, and 5 cells were randomly selected from each image to record the fluorescence intensity. Therefore, each treatment included 30 sets of data.

Determination of calcium in BPH

One-day-old BPH females (reared on susceptible rice seedlings, of rice variety Huang Huazhan) were reared in feeding chambers, and the rearing procedure followed that described by Fu *et al.* (2001). Briefly, the females were kept in the feeding chambers for 4 h for adaption to the environment with no food or water. After that, the parafilm was replaced and filled with galactose solution or ddH_2O with 0.2% w/v Brilliant Blue FCF. Every 10 females with a light-blue abdomen were collected in a 1.5-mL *EP* tubes to detect the Ca^{2+} level using an ELISA kit (GenMed, Cwmbran, Wales, UK), following the manufacturer's instructions, after 5, 10, 20, 30, 60, 120, and 180 min. After obtaining the optical density (OD 570 nm) values of these test samples by using the kit, we calculated the actual Ca^{2+} level in the test samples according to the standard curve based on the standard samples. Each treatment included 8 biological replicates.

Electrical penetration graph (EPG) recording of BPH feeding behavior

The feeding behavior of the BPHs was recorded on a Giga-8 DC EPG amplifier (GDAAS, Guangdong, China), based on a previously described method (Zhang *et al.*, 2015). Briefly, all experiments were conducted at 26 ± 1°C and 70% ± 10% relative humidity under continuous light conditions. The feeding behavior of individual BPHs on galactose solution was monitored for 3 h. For each treatment, 20 biological replications were conducted, and the signals recorded were analyzed using PROBE 3.0. Each feeding behavior was expressed as the proportion of each waveform duration (%) and the number of each waveform occurrences. The frequency and time of the PW, N3, and N4 waves were analyzed. The PW, N3, and N4 waves represent probing, saliva secretion, and feeding, respectively.

Determination of feeding amount of BPH

As it is impossible to directly quantify the feeding loads of BPHs, we utilized the ingestion assay. The ingestion assay was performed as previously described (Sang *et al.*, 2019), with some modifications. One-day-old BPH females (reared on susceptible rice seedlings, of rice variety Huang Huazhan) were reared in feeding chambers. The females were kept in feeding chambers for 4 h for starvation and adaption to the environment, with no food or water. After that, the parafilm was replaced and filled with galactose solution or ddH_2O and 0.2% w/v Brilliant Blue FCF to feed the females. Three hours later, the females were transferred into a 1.5-mL EP tube filled with 500 μL PBST (1× PBS with 0.2% Triton X-100) and completely ground. Each tube contained 10 females. The tube was centrifuged for 10 min at 15 000 × *g*

at 4°C. Lastly, the supernatant was loaded in cuvettes for a spectrophotogram measured at 630 nm and the ingestion index (I.I.) was calculated. The formula for I.I. is $(O.D._{galactose\_diet} - O.D._{control\_diet})/(O.D._{control\_diet})$. Each treatment include 10 biological replicates.

Determination of NlVg by Western blot

One-day-old BPH females (reared on susceptible rice seedlings, of rice variety Huang Huazhan) were reared in feeding chambers. The parafilm was filled with galactose solution or ddH_2O. Seventy-two hours later, the females were collected, and the total protein was extracted from 4 females in each of the 3 replicates performed. The whole bodies were lysed in 1× Passive Lysis Buffer. The homogenate was centrifuged at 12 000 × *g* at 4°C for 15 min, and the protein content in the supernatants was measured by the Bradford method. The Western blot technique was modified according to previously described methods (Mitsumasu *et al.*, 2008). In this study, 20 μg of total protein was separated on a 10% sodium dodecyl sulfate polyacrylamide gel electrophoresis (SDS-PAGE) gel and transferred to polyvinylidene fluoride (PVDF) membranes (0.45 μm; Millipore, Burlington, MA, USA), and the membranes were immunoblotted with anti-*Nl*Vg (1 : 500; Abmart, Berkeley Heights, NJ, USA) and anti-β-actin (1 : 4000; Abcam, Boston, MA, USA). The secondary antibody was IgG goat anti-rabbit conjugated to horseradish peroxidase (HRP) (1 : 5000; Cell Signaling Technology, Danvers, MA, USA). The membranes were visualized using ECL (Millipore) and Image Lab (Bio-Rad, Hercules, CA, USA). The protein bands were quantified by importing the images into ImageJ analysis software (Wayne Rasband, National Institutes of Health, Bethesda, MD, USA).

Statistical analysis

We performed all statistical analyses using SPSS Statistics 17 (IBM, Armonk, NY, USA). All data were expressed as means (SEMs). Differences between 2 means were analysed using a Student's *t*-test, and differences among multiple groups were analysed using one-way analysis of variance (ANOVA) followed by the Duncan's multiple range test for multiple comparisons. Differences with $P < 0.05$ were considered statistically significant and were marked with an asterisk (*) or with different letters.

Results

Activation of signaling pathways by galactose-NlGr11 based on galactose concentrations in vitro and in vivo

Insect gustatory receptor–ligand binding often leads to a significant increase of intracellular Ca^{2+}. To investigate the mechanism of the increase in intracellular Ca^{2+} level mediated by galactose-*Nl*Gr11, we added 50 mmol/L (saturated concentration) galactose solution to *Nl*Gr11-*Sf*9 cells and *Sf*9 cells incubated with Hank's solution (with Ca^{2+}) or D-Hank's solution (without Ca^{2+}), and changes in intracellular Ca^{2+} level were tested by calcium imaging assay. The results showed that intracellular Ca^{2+} levels increased significantly in *Nl*Gr11-*Sf*9 cells incubated with Hank's and D-Hank's (Fig. 1A). The rise in the intracellular Ca^{2+} level was independent of extracellular Ca^{2+} presence, suggesting a release of Ca^{2+} from intracellular stores. Subsequently, we found that GDP-βS, an inhibitor of the G protein-coupled signaling pathway, significantly inhibited the *Nl*Gr11-mediated Ca^{2+} responses induced by galactose (Fig. 1B). In *Sf*9 cells, the intracellular Ca^{2+} levels were not changed significantly when cells were treated with galactose, Hank's, D-Hank's, or GDP-βS (Figs. S1 and S2). These results implied that the rise in Ca^{2+} level mediated by galactose-*Nl*Gr11 occurs via the G protein-coupled signaling pathway *in vitro*.

In addition, compared with the D-Hank's group (latency of 19 s, decay of 15 s, and maximum Ca^{2+} level of 1.86), the Ca^{2+} response in the Hank's group develops faster but decays slower and is considerably greater (latency of 4 s, decay of 28 s, and maximum Ca^{2+} level of 2.68) (Fig. 1D). We also found that the Ca^{2+} level still increased in the Hank's group after treatment with GDP-βS (Fig. 1B, E), suggesting that the Ca^{2+} influx occurs through the opening of ion channels mediated by galactose-*Nl*Gr11. Therefore, we loaded manidipine 2HCl, an ion channel inhibitor, into *Nl*Gr11-*Sf*9 cells and performed a calcium imaging assay. We found no significant difference the in Ca^{2+} response mediated by galactose-*Nl*Gr11 between the Hank's and D-Hank's groups (Fig. 1C, F). The intracellular Ca^{2+} levels of *Sf*9 cells were not changed significantly when the cells were treated with manidipine 2HCl (Fig. S2). Therefore, the rise in Ca^{2+} level mediated by galactose-*Nl*Gr11 is also mediated through an influx of Ca^{2+} via the ionotropic pathway.

Subsequently, we investigated the Ca^{2+} responses, mediated by *Nl*Gr11, to unsaturated galactose concentrations (5, 10, 20, 40, and 45 mmol/L). The results demonstrated that the Ca^{2+} level in the D-Hank's group did not change significantly but was increased significantly in

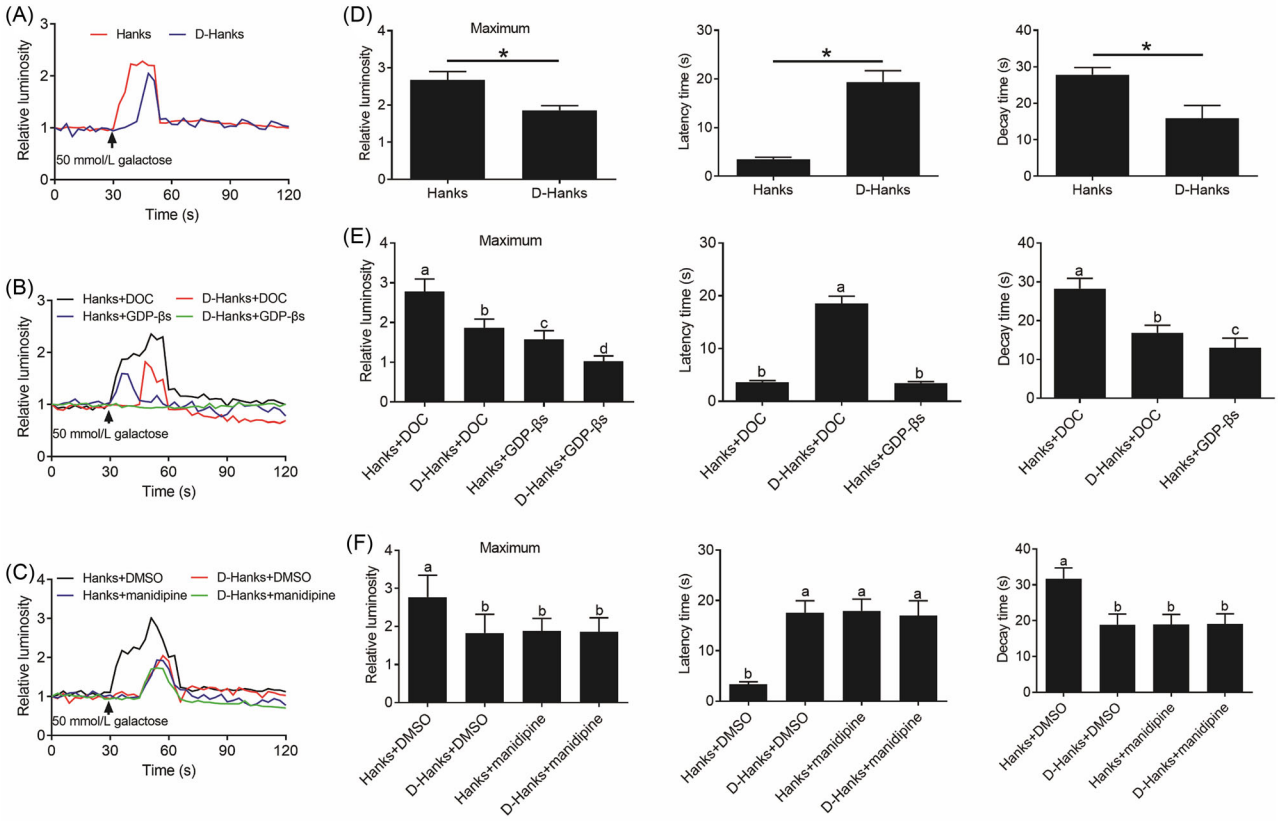

Fig. 1 *Nl*Gr11-mediated Ca^{2+} responses induced by a saturated concentration of galactose solution in *Nl*Gr11-*Sf*9 cells. (A) Ca^{2+} responses in Hank's solution (with Ca^{2+}) and D-Hank's solution (without Ca^{2+}) mediated by galactose-*Nl*Gr11. (B) Inhibition of Ca^{2+} response to galactose in the cells by GDP-βS. The cells were pretreated with 100 μL of 0.03% DOC (dissolved in 67 mmol/L phosphate buffer, pH 7.2) for 4 min, and then treated with GDP-βS (2 mmol/L) for 4 min. DOC was used to introduce GDP-βS into the cells. (C) Inhibition of Ca^{2+} response to galactose in the cells by manidipine 2HCl (3 nmol/L) for 10 min. Relative luminosity represents the level of intracellular Ca^{2+}; the value was set to 1 before adding a galactose solution of 50 mmol/L. (D–F) Maximum represents the maximum Ca^{2+} concentration; latency time is the time when the Ca^{2+} level starts to increase after the addition of galactose solution; decay time is the duration of Ca^{2+} responses after the addition of galactose solution. The data in (A–C) represent means ($N = 30$); the data in (D–F) represent means ± SEMs ($N = 30$). (D) *$P < 0.05$, Student's *t*-test. (E, F) Different lowercase letters above bars indicate significant differences ($P < 0.05$, Duncan's multiple range test). DOC, deoxycholate; SEM, standard error of the mean.

the Hank's group (Fig. 2A–E). In addition, when *Nl*Gr11-*Sf*9 cells were pretreated with manidipine 2HCl, the intracellular Ca^{2+} level in the Hank's group did not change significantly (Fig. 2F). The intracellular Ca^{2+} levels of *Sf*9 cells were not changed significantly when the cells were treated with different concentrations of galactose solution (Fig. S1). These results reveal that the mechanism for the rise in intracellular Ca^{2+} level depends on the concentration of the galactose solution. *Nl*Gr11-mediated Ca^{2+} responses induced by the saturated concentration (50 mmol/L) of galactose simultaneously activated G protein-coupled signaling and ionotropic pathways, whereas unsaturated galactose concentrations activated only the ionotropic pathway *in vitro*.

We also confirmed the results of the above cell experiments in BPH. After BPHs were fed with galactose solutions, we found that the Ca^{2+} level increased with the increase in the concentration of galactose (Fig. 3A). Moreover, we identified that when BPH were fed on 100 mmol/L galactose solution (latency of 5 min, decay of 175 min, and maximum Ca^{2+} level of 2.94), the Ca^{2+} response developed to a maximum and then decayed more slowly than that in BPHs fed on other concentrations of galactose (latency of 5 min, decay of 55 min, and maximum Ca^{2+} levels of 1.83 for 5 mmol/L, 2.04 for 20 mmol/L, and 2.23 for 50 mmol/L) (Fig. 3). These results were similar to those obtained in the above cell experiments and

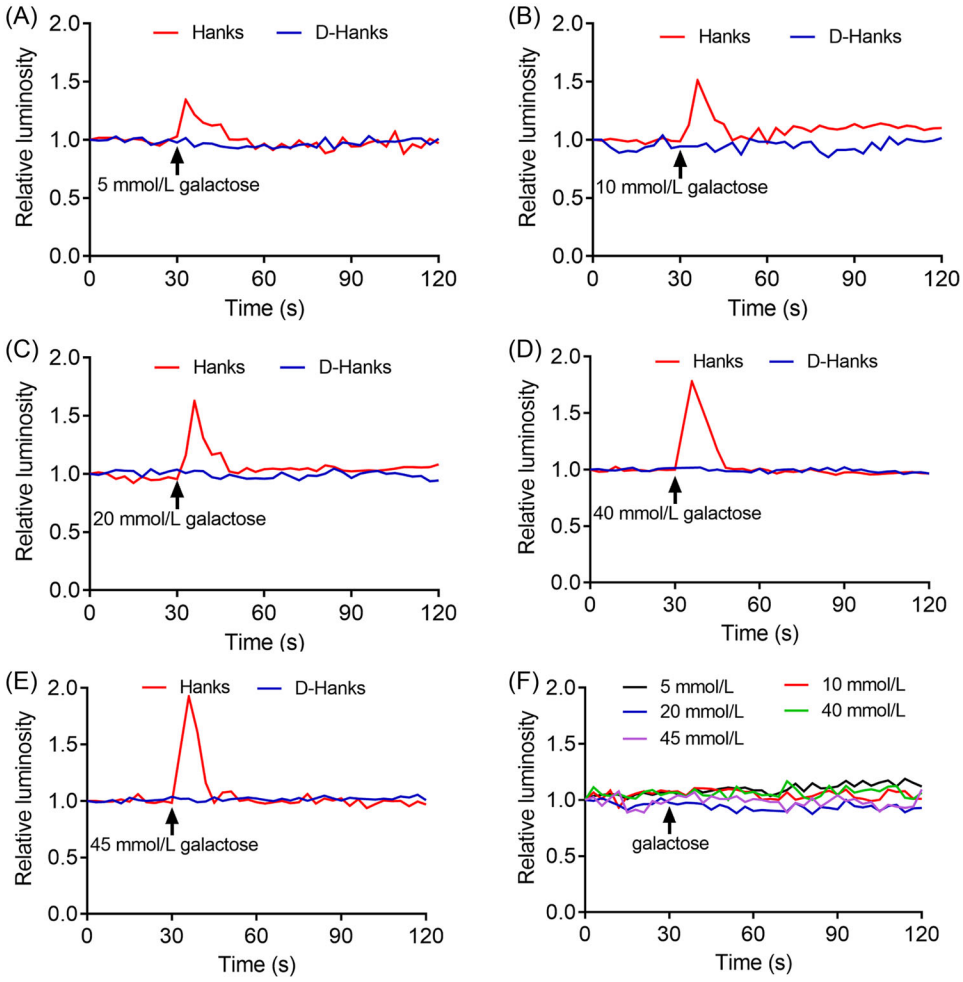

Fig. 2 *Nl*Gr11-mediated Ca^{2+} responses induced by unsaturated concentrations of galactose solution in *Nl*Gr11-*Sf*9 cells. Ca^{2+} responses in Hank's solution (with Ca^{2+}) and D-Hank's solution (without Ca^{2+}) induced by galactose solutions of 5 mmol/L (A), 10 mmol/L (B), 20 mmol/L (C), 40 mmol/L (D), and 45 mmol/L (E). (F) Inhibition of the Ca^{2+} response to unsaturated galactose concentrations in the cells by manidipine 2HCl (3 nmol/L) for 10 min. Relative luminosity represents the level of intracellular Ca^{2+}; the value was set to 1 before adding galactose solution. Data represent means ($N = 30$).

indicated that feeding BPH with 100 mmol/L galactose solution activated both the G protein-coupled signaling and ionotropic pathways, whereas feeding BPH with 50 mmol/L galactose activated only the ionotropic pathway.

Lastly, we examined whether galactose-*Nl*Gr11 activated the G protein–PLCβ–IP3 signaling cascade. The results demonstrated that U73122, an inhibitor of phospholipase C (PLC) activation, significantly inhibited the Ca^{2+} response mediated by galactose-*Nl*Gr11 (Fig. 4A). After loading an IP3-gated channel antagonist (2-APB) and agonist (adenophostin A) into the cells, we observed that 2-APB significantly inhibited the Ca^{2+} response mediated by galactose-*Nl*Gr11 (Fig. 4B), and that adenophostin A resulted in the opposite effect (Fig. 4C). The intracellular Ca^{2+} levels of *Sf*9 cells did not change significantly when the cells were treated with U73122, 2-APB, or adenophostin A (Fig. S2). These results suggest that galactose-*Nl*Gr11 activated the Gq–PLCβ–IP3 signaling cascade. We also showed that BPHs fed on 100 mmol/L galactose solution had a significant increase in IP3 levels (Fig. 4D). This behavior confirmed that 100 mmol/L galactose solution activated both G protein-coupled signaling and ionotropic pathways, whereas 50 mmol/L galactose solution only activated the ionotropic pathway *in vivo*.

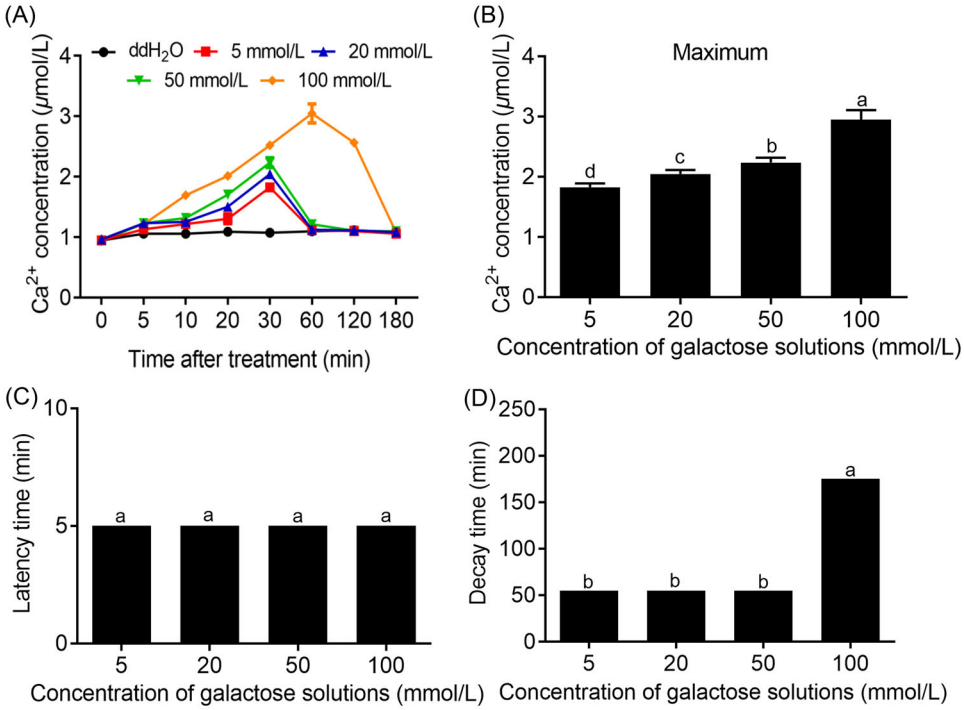

Fig. 3 Ca^{2+} responses mediated by galactose-*Nl*Gr11 in the BPH. (A) The Ca^{2+} level of BPHs after feeding on galactose solutions of 5, 20, 50, and 100 mmol/L. (B) The maximum Ca^{2+} concentration. (C) The time when the Ca^{2+} level starts to increase after the addition of galactose solution. (D) The duration of the Ca^{2+} responses after the addition of galactose solution. Data represent means ± SEMs ($N = 8$). The different lowercase letters above the bars indicate significant differences ($P < 0.05$, Duncan's multiple range test). BPH, brown planthopper; SEM, standard error of the mean.

Galactose dose-dependent feeding efficacy and NlVg expression in BPH

To investigate whether various signaling pathways activated by 2 galactose concentrations affect the physiological functions of BPHs, we performed an EPG to analyze the BPH feeding process. The results showed that the feeding times on 50 mmol/L galactose solution were longer than the feeding times on 100 mmol/L galactose (Fig. 5A). During the test period, BPHs only fed 3 times at most on 100 mmol/L galactose solution (data not shown), so we compared and analyzed the feeding process of the first 3 rounds. During each feeding round, no difference was found in the probing time of BPHs (Fig. 5B), but when BPHs were fed on 100 mmol/L galactose solution, the saliva secretion time and feeding time of the BPHs were significantly longer than in BPHs fed on 50 mmol/L galactose (Fig. 5C, D). Subsequently, we analyzed the feeding load of BPHs, and because this is impossible to quantify directly, we used an ingestion assay to calculate the I.I. to represent the feeding amount. The results showed that the I.I. of BPHs fed on 100 mmol/L galactose solution was 1.66, significantly higher than the I.I. of BPHs fed on 50 mmol/L galactose solution (Fig. 5E). Therefore, when *Nl*Gr11 recognized a low galactose concentration, the BPHs spent less time feeding and subsequently obtained less food, whereas with a high galactose concentration the BPHs showed higher feeding efficacy.

We also analyzed the protein expression level of *Nl*Vg, a molecular marker of insect fecundity, after feeding BPHs with galactose solutions of 50 and 100 mmol/L. We found that the *Nl*Vg level in BPHs when the BPHs were fed on 100 mmol/L galactose solution was significantly higher than in BPHs fed on 50 mmol/L galactose (Fig. 5F). This suggests that feeding on a high concentration of galactose increased the *Nl*Vg level and is likely to increase the fecundity of the BPHs.

Discussion

In the field, insects are often exposed to both conditions with sufficient nutrients and conditions of undernutrition. Here, using galactose as an example, for the first time

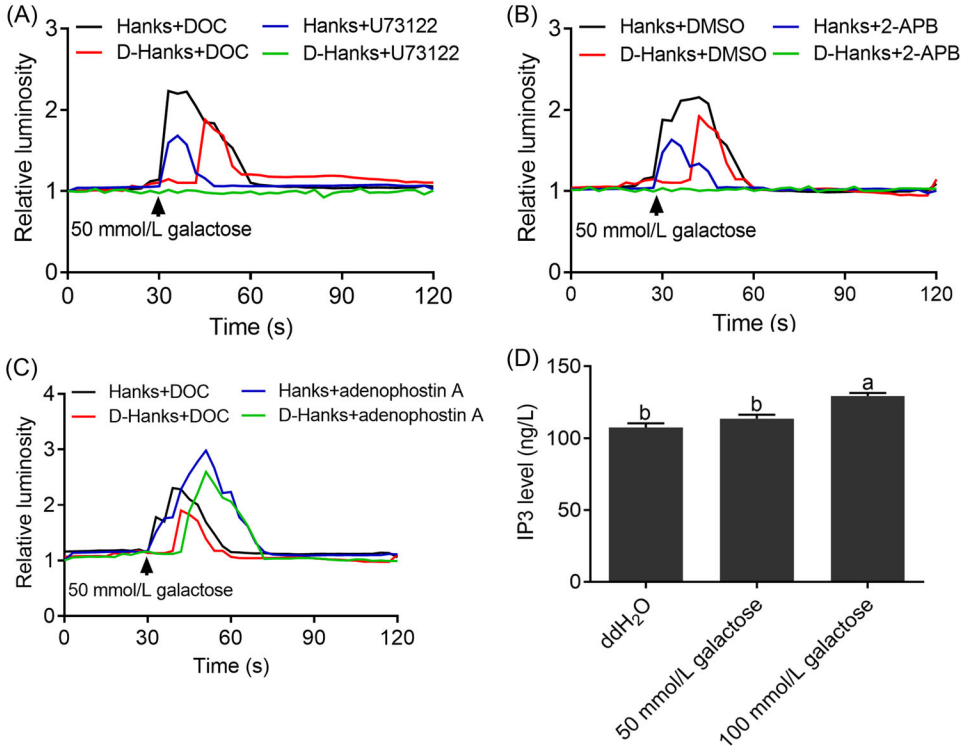

Fig. 4 Galactose-*Nl*Gr11 activates the Gq–PLCβ–IP3 signaling cascade. (A) Inhibition of Ca^{2+} response to a galactose solution of 50 mmol/L in the cells by U73122. The cells were pretreated with 100 μL of 0.03% DOC (dissolved in 67 mmol/L phosphate buffer, pH 7.2) for 4 min, and then treated with U73122 (0.025 mmol/L) for 8 min. (B) Inhibition of Ca^{2+} response to a galactose solution of 50 mmol/L in the cells by 2-APB (1 mmol/L). 2-APB (1 mmol/L) was added into the cells for 8 min. (C) Promotion of Ca^{2+} response to a galactose solution of 50 mmol/L in the cells by adenophostin A. The cells were pretreated with 100 μL of 0.03% DOC (dissolved in 67 mmol/L phosphate buffer, pH 7.2) for 4 min, and then treated with adenophostin A (1 mmol/L) for 1 min. Relative luminosity represents the level of intracellular Ca^{2+}; the value was set to 1 before adding the galactose solution. Data in (A–C) represent means ($N = 30$). (D) The IP3 level of BPHs after feeding on galactose solutions of 50 and 100 mmol/L. Data represent means ± SEM ($N = 5$). Different lowercase letters above the bars indicate significant differences ($P < 0.05$, Duncan's multiple range test). 2-APB, 2-aminoethoxydiphenylborate; BPH, brown planthopper; DOC, deoxycholate; SEM, standard error of the mean.

we have linked plant nutrient conditions, signaling pathways activated by nutrients, and their gustatory receptors, and nutrient dose-dependent feeding efficacy and fecundity in an insect. We found that saturated galactose concentration activated both G protein-coupled signaling and ionotropic pathways and subsequently increased feeding efficacy and Vg expression in BPHs, whereas feeding on a low galactose concentration activated only the latter pathway and the BPHs exhibited lower feeding efficacy and Vg expression.

One of our significant findings is that galactose-*Nl*Gr11 activates the ionotropic pathway independently of galactose concentration and exhibits a speedy response. It indicates that *Nl*Gr11 ensures very rapid recognition and high sensitivity to low galactose concentrations through the ionotropic pathway. Although *Bm*Gr9 and *Bm*Gr10 also activate the ionotropic pathway, it is not clear whether this is related to their ligand concentration (Sato *et al.*, 2011; Kikuta *et al.*, 2016). Together with the results of *Bm*Gr9 and *Bm*Gr10, insect gustatory receptors seem to transmit signals initially through the ionotropic pathway. One important function of insect gustatory receptors is to help insects recognize food (Chapman, 2003). Therefore, we speculate that insect gustatory receptors transmit food information to the brain mainly by activating the ionotropic pathway after recognizing food. As a result of the rapid response and high sensitivity of the ionotropic pathway, insects may be able to judge the nutritional value of food in a very short time through their gustatory receptors and the ionotropic pathway, and so can choose more suitable food for feeding.

Another important finding is that the G protein-coupled signaling pathway is only activated by galactose-*Nl*Gr11 when the galactose concentration is high enough,

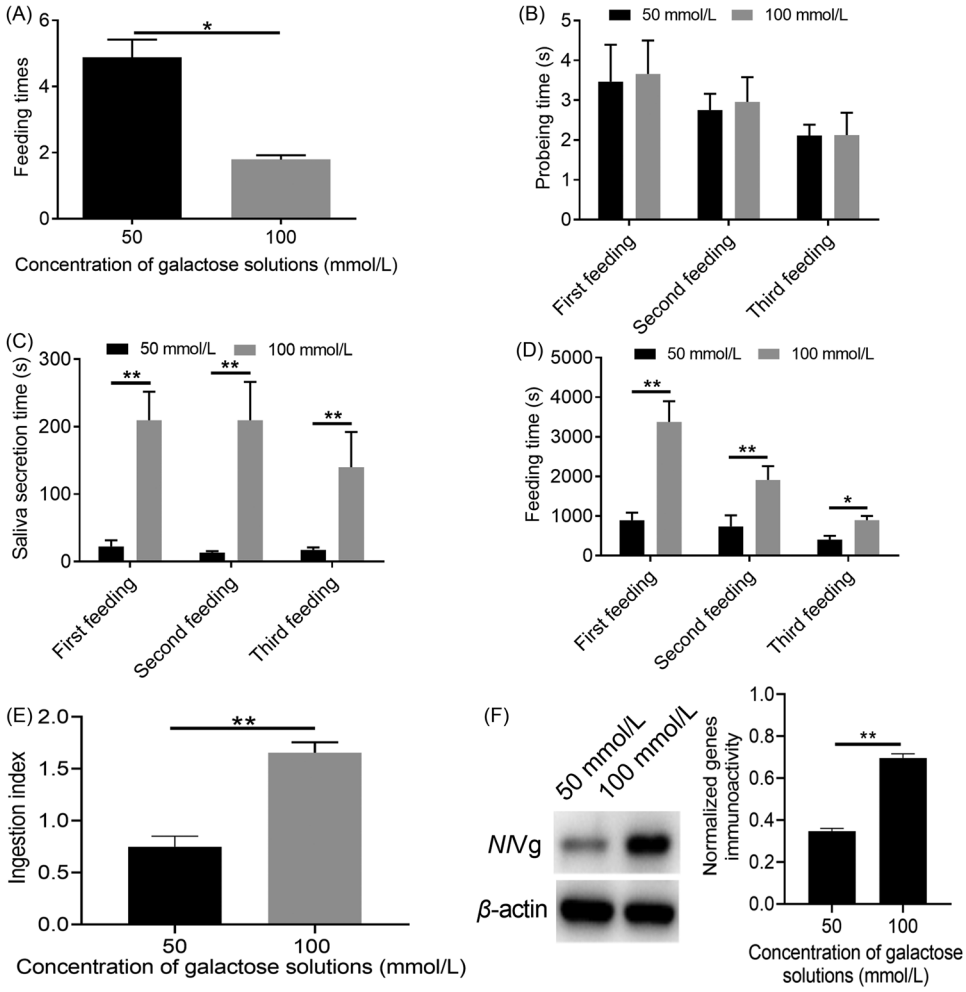

Fig. 5 Feeding processes of BPHs fed on galactose solutions of 50 and 100 mmol/L: number of feeds (A), probing time (B), saliva secretion time (C), and feeding time (D) during the 3 periods of feeding and ingestion index (E) of BPHs feeding on galactose solutions of 50 and 100 mmol/L. (F) The protein levels of *Nl*Vg after feeding BPHs with galactose solutions of 50 and 100 mmol/L. All measurements were normalized to β-actin protein levels. Data represent means ± SEMs. (A–C) $N = 20$. (D) $N = 8$. (F) $N = 3$. $^{*}P < 0.05$, $^{**}P < 0.01$, Student's *t*-test. BPH, brown planthopper; SEM, standard error of the mean.

and the response is somewhat slower but is larger and prolonged. Until now, no other insect gustatory receptors that activate the G protein-coupled signaling pathway have been found. Although mammalian sweet and bitter taste receptors activate the G protein-coupled signaling pathway (Roper & Chaudhari, 2017), it is unknown whether this is related to ligand concentration. The slow response of the G protein-coupled signaling pathway suggests that gustatory receptors are not likely to perceive food through this pathway. This is consistent with our finding for the probing time of BPHs fed on galactose solutions of 50 and 100 mmol/L; that is, the time to perceive food does not differ and is short, regardless of whether the G protein-coupled signaling pathway is activated or not (Fig. 5B). However, BPHs showed fewer feeds, longer feeding times, and greater feeding loads when the G protein-coupled signaling pathway was activated (Fig. 5A–D). This demonstrates that the G protein-coupled signaling pathway may play a role in regulating the efficacy of insect feeding. In mammals, sweet receptors increase intracellular Ca^{2+} levels through the G protein-coupled signaling pathway, and increased Ca^{2+} triggers neurotransmitter release and transmits signals to the central nervous system (Ahmad & Dalziel, 2020). Therefore, insects receive stronger and more prolonged taste signals through the G protein-coupled signaling pathway, leading to higher feeding efficacy. As feeding is fundamental for insect growth and reproduction,

insect gustatory receptors may regulate more physiological functions through the G protein-coupled signaling pathway. In this study, upon activation of the G protein-coupled signaling pathway, the protein expression level of *Nl*Vg is higher (Fig. 5F). An artificial feeding method was used to feed the BPHs with galactose solution, and it was impossible to count the number of eggs laid and the hatching rate of the eggs, so we only detected the protein level of Vg, a molecular marker of insect fecundity (Qiu *et al.*, 2016; Pang *et al.*, 2017). Therefore, we suppose that high galactose concentration enhanced the feeding efficacy and increased the *Nl*Vg level, and is therefore likely to increase the fecundity of the BPHs.

Despite these promising results, some questions remain unanswered. First, the mechanism by which galactose-*Nl*Gr11 activates the ionotropic pathway and the G protein-coupled signaling pathway is unclear. *Nl*Gr11 is expressed in various tissues of BPHs (Chen *et al.*, 2019). Therefore, one alternative hypothesis is that *Nl*Gr11 expressed in different tissues may contact different concentrations of galactose and activate different signaling pathways for regulating different biochemical or physical responses. In addition, *Nl*Gr11 possess 7 transmembrane domains, as well as the N-terminal inside the membrane and the C-terminal outside the membrane (Fig. S3), which is contrary to the traditional G protein-coupled receptor (GPCR) structure. Moreover, we did not find the G protein binding domain when we analyzed the protein structure of *Nl*Gr11 through the Pfam website and other websites or software (data not shown). Therefore, another alternative hypothesis is that *Nl*Gr11 may be able to bind to other GPCRs. When *Nl*Gr11 binds to the ligand, the conformation of GPCR will change, thus activating the G protein-coupled signaling pathway. At present, it is known that some insect gustatory receptors form multimeric complexes to sense taste substances (Jiao *et al.*, 2007; Jung *et al.*, 2015). Therefore, we speculate that galactose-*Nl*Gr11 activating the ionic pathway through *Nl*Gr11 interacting with ionic taste receptors or *Nl*Gr11 itself has the conformation to activate ion channels. Second, we are skeptical as to whether signaling pathways activated by other insect gustatory receptors also depend on ligand concentration. Although *Bm*Gr9 and *Bm*Gr10 have been reported not to activate the G protein-coupled signaling pathway (Sato *et al.*, 2011; Kikuta *et al.*, 2016), only 1 concentration of a taste substance was investigated, and so it cannot be ruled out that, like *Nl*Gr11, the G protein-coupled signaling pathway will be activated when the concentration of the taste substance is higher or lower. Finally, because insect gustatory receptors frequently have more than 1 ligand, signaling pathways activated by gustatory receptors may be related to ligand types in addition to dose dependence. We believe that these are topics that require further study in the future.

Acknowledgments

We are grateful to Dr. Longyu Yuan and Mr. Gu Gong from Guangdong Academy of Agricultural Sciences for their help with the EPG experiment. This work was supported by the National Natural Science Foundation of China (31730073, U1401212) and Guizhou Science and Technology Project (qiankeheji-zk [2021] General 135).

Disclosure

The authors declare that they have no conflicts of interest associated with this work.

References

Ahmad, R. and Dalziel, J.E. (2020) G protein-coupled receptors in taste physiology and pharmacology. *Frontiers in Pharmacology*, 11, 587664.

Ai, D., Dong, C.X., Yang, B., Yu, C.H. and Wang, G.R. (2022) A fructose receptor gene influences development and feed intake in *Helicoverpa armigera*. *Insect Science*, 29, 993–1005.

Bi, J.L., Ballmer, G.R., Hendrix, D.L., Henneberry, T.J. and Toscano, N.C. (2001) Effect of cotton nitrogen fertilization on *Bemisia argentifolii* populations and honeydew production. *Entomologia Experimentalis et Applicata*, 99, 25–36.

Chapman, R.F. (2003) Contact chemoreception in feeding by phytophagous insects. *Annual Review of Entomology*, 48, 455–484.

Chen, W.W., Kang, K., Lv, J., Yue, L. and Zhang, W.Q. (2021) Galactose-*Nl*Gr11 inhibits AMPK phosphorylation by activating the PI3K-AKT-PKF-ATP signaling cascade via insulin receptor and G$\beta\gamma$. *Insect Science*, 28, 735–745.

Chen, W.W., Kang, K., Yang, P. and Zhang, W.Q. (2019) Identification of a sugar gustatory receptor and its effect on fecundity of the brown planthopper *Nilaparvata lugens*. *Insect Science*, 26, 441–452.

Du, B., Zhang, W.L., Liu, B.F., Hu, J., Wei, Z., Shi, Z.Y. *et al.* (2009) Identification and characterization of *Bph14*, a gene conferring resistance to brown planthopper in rice. *Proceedings of the National Academy of Sciences USA*, 106, 22163–22168.

Facknath, S. and Lalljee, B. (2005) Effect of soil-applied complex fertiliser on an insect–host plant relationship: *Liriomyza trifolii* on *Solanum tuberosum*. *Entomologia Experimentalis et Applicata*, 115, 67–77.

Fischer, K. and Fiedler, K. (2000) Response of the copper butterfly *Lycaena tityrus* to increased leaf nitrogen in natural

food plants: evidence against the nitrogen limitation hypothesis. *Oecologia*, 124, 235–241.

Fu, Q., Zhang, Z., Hu, C., Lai, F.X. and Sun, Z.X. (2001) A chemically defined diet enables continuous rearing of the brown planthopper, *Nilaparvata lugens* (Stål) (Homoptera: Delphacidae). *Applied Entomology and Zoology*, 36, 111–116.

Jiao, Y.C., Moon, S.J. and Montell, C. (2007) A *Drosophila* gustatory receptor required for the responses to sucrose, glucose, and maltose identified by mRNA tagging. *Proceedings of the National Academy of Sciences USA*, 104, 14110–14115.

Jung, J.W., Park, K.W., Ahn, Y.J. and Kwon, H.W. (2015) Functional characterization of sugar receptors in the western honeybee, *Apis mellifera*. *Journal of Asia-Pacific Entomology*, 18, 19–26.

Kikuta, S., Endo, H., Tomita, N., Takada, T., Morita, C., Asaoka, K. *et al*. (2016) Characterization of a ligand-gated cation channel based on an inositol receptor in the silkworm, *Bombyx mori*. *Insect Biochemistry and Molecular Biology*, 74, 12–20.

Lastdrager, J., Hanson, J. and Smeekens, S. (2014) Sugar signals and the control of plant growth and development. *Journal of Experimental Botany*, 65, 799–807.

Li, J.L., Zhang, X.Y., Du, Y.D., Wang, H., Wu, L.J. and Hu, F. (2013) Effects of high temperature on rice source-sink characteristics during heading stage to grain filling stage. *Zhonghua Nongye Qixiang*, 34, 23–29.

Lin, X.D., Xu, Y.L., Jiang, J.R. Lavineb, M. and Lavine, L.C. (2018) Host quality induces phenotypic plasticity in a wing polyphenic insect. *Proceedings of the National Academy of Sciences USA*, 115, 7563–7568.

Mitsumasu, K., Azuma, M., Niimi, T., Yamashita, O. and Yaginuma, T. (2008) Changes in the expression of soluble and integral-membrane trehalases in the midgut during metamorphosis in *Bombyx mori*. *Zoological Science*, 25, 693–698.

Miyamoto, T., Slone, J., Song, X.Y. and Amrein, H. (2012) A fructose receptor functions as a nutrient sensor in the *Drosophila* brain. *Cell*, 151, 1113–1125.

Naziri, A.M., Kassim, N.F.A., Jong, Z.W. and Webb, C.E. (2016) Effects of sugar concentration on fecundity, biting behavior and survivability of female *Aedes* (stegomyia) *albopictus* (Skuse). *The Southeast Asian Journal of Tropical Medicine and Public Health*, 47, 1160–1116.

Nevo, E. and Coll, M. (2001) Effect of nitrogen fertilization on *Aphis gossypi* variation in size, color, and reproduction. *Journal of Economic Entomology*, 94, 27–32.

Ortego, F. (2012) Physiological adaptations of the insect gut to herbivory. In: *Arthropod–Plant Interactions Novel Insights and Approaches for IPM* (eds. G. Smagghe & I. Diaz), pp. 15–73. Springer, Dordrecht.

Pang, R., Qiu, J.Q., Li, T.C., Pan, Y.X., Yue, L., Yang, P. *et al*. (2017) The regulation of lipid metabolism by a hypothetical P-loop NTPase and its impact on fecundity of the brown planthopper. *Biochimica et Biophysica Acta – General Subjects*, 1861, 1750–1758.

Qiu, J.Q., He, Y., Zhang, J.Q., Kang, K., Li, T.C. and Zhang, W.Q. (2016) Discovery and functional identification of fecundity-related genes in the brown planthopper by large-scale RNA interference. *Insect Molecular Biology*, 25, 724–733.

Roper, S.D. and Chaudhari, N. (2017) Taste buds: cells, signals and synapses. *Nature Reviews Neuroscience*, 18, 485–497.

Sato, K., Tanaka, K. and Touhara, K. (2011) Sugar-regulated cation channel formed by an insect gustatory receptor. *Proceedings of the National Academy of Sciences USA*, 108, 11680–11685.

Sang, J., Rimal, S. and Lee, Y. (2019) Gustatory receptor 28b is necessary for avoiding saponin in *Drosophila melanogaster*. *EMBO Reports*, 20, e47328.

Sōgawa, K. (1982) The rice brown planthopper: feeding physiology and host plant interactions. *Annual Review of Entomology*, 27, 49–73.

Williams, L., Deschodt, P., Pointurier, O. and Wyckhuys, K.A. (2015) Sugar concentration and timing of feeding affect feeding characteristics and survival of a parasitic wasp. *Journal of Insect Physiology*, 79, 10–18.

Xu, W. (2020) How do moth and butterfly taste?—Molecular basis of gustatory receptors in Lepidoptera. *Insect Science*, 27, 1148–1157.

Yang, L. and Zhang, W.L. (2016) Genetic and biochemical mechanisms of rice resistance to planthopper. *Plant Cell Reports*, 35, 1559–1572.

Zhang, Z.F., Cui, B.Y. and Zhang, Y. (2015) Electrical penetration graphs indicate that tricin is a key secondary metabolite of rice, inhibiting phloem feeding of brown planthopper, *Nilaparvata lugens*. *Entomologia Experimentalis et Applicata*, 156, 14–27.

Manuscript received October 5, 2022
Final version received December 12, 2022
Accepted January 4, 2023

Supporting Information

Additional supporting information may be found online in the Supporting Information section at the end of the article.

Fig. S1 Ca^{2+} responses induced by different concentrations of galactose solution in *Sf*9 cells.

Fig. S2 Ca^{2+} responses induced by some chemicals and a saturated concentration of galactose solution in *Sf*9 cells.

Fig. S3 Transmembrane structure analysis of *Nl*Gr11.